Band Textures of Liquid Crystalline Polymers in Elongational Flows

Edith Peuvrel and Patrick Navard*

Centre de Mise en Forme des Matériaux, URA CNRS 1374, Ecole Nationale Supérieure des Mines de Paris, Sophia-Antipolis, 06560 Valbonne, France

Received January 29, 1991; Revised Manuscript Received May 20, 1991

ABSTRACT: A rheooptical device, where an obstacle generates an elongational flow, was used to study the behavior of an anisotropic (hydroxypropyl)cellulose solution. Good agreement was found between calculated and measured elongational rates. After cessation of flow, a band texture appears if the elongation rate is larger than a critical value. The conditions for the formation of the bands, their optical features, and their spacing are similar to those arising after cessation of shear.

Liquid crystalline polymers after cessation of shear or elongation may exhibit under particular conditions a characteristic texture called "band texture". This texture consists of fine equidistant black lines (viewed between crossed polarizers with one polarizer parallel to the flow direction) that are perpendicular to the flow direction. Bands have been observed with many different mesomorphic polymers such as lyotropic, thermotropic, nematic, or cholesteric at rest systems.

The band texture observed after cessation of shear has been extensively studied. It appears that this texture originates from a serpentine position of the director along the flow direction.[1-3] The conditions for the formation of bands are such that bands only appear above a minimum shear rate and a minimum shear deformation (a minimum shearing time).[4-8] The spacing between two bands depends on the fluid concentration[9] but is independent of the shear conditions[5,9] or of the sample depth.[5,9] Even if the conditions for the formation of bands after a shear are well understood, the origin of these bands is still unknown.

The circumstances for the band texture appearing after an elongation are less clear. It is known that a band texture might appear after drawing a fiber from a liquid crystalline polymer,[10,11] but due to the difficulty of performing a steady-state elongation experiment, no data are presently available concerning the conditions for the formation of this texture. There is no comparison either between the band texture after a shear or after an elongation for the same polymer.

The purpose of this paper is to study the formation of a band texture after an elongation for an anisotropic (hydroxypropyl)cellulose solution and to compare it to the known case of shear.

Experimental Section

The aim of the study implies the possibility of observing visually the flow and the relaxation of the solution after an elongation. This condition rules out any method linked to drawing a filament, either during spinning or in an elongational rheometer.

During the course of another study,[12,13] we built an experimental setup consisting of a transparent cone-and-plate rheometer with a glass sphere glued on the plate, which acts as a near-cylindrical obstacle. Behind such an obstacle any fluid is submitted to an elongational flow.[14] This tool allows rheooptical observations to be performed.

As will be stressed in the next section, this geometry has several drawbacks linked to the presence of a shear component. This would be the case for any other device (contraction flow, opposed slot flow, etc.) since the transparency of these anisotropic fluids is very limited and thus imposed a low thickness.

The obstacle is a 250-μm glass sphere stuck on the plate. The gap where the glass sphere stands is about 350 μm. A detailed description of the setup is given in ref 13. The observations were performed with an optical microscope between crossed polarizers, the analyzer being parallel to the flow direction.

An anisotropic (hydroxypropyl)cellulose (Hercules Klucel)–water solution (M_w = 100 000, concentration 55% by weight) was prepared by the usual procedure,[5,6] except that a few percent was filled with well-calibrated polystyrene spheres (diameter 9.89 μm, National Bureau of Standards reference material no. 1960). The spheres were used as velocity tracers. We checked that the moving spheres did not perturb the flow and could be considered as moving at the same speed as the surrounding fluid.[15]

In the vicinity of the obstacle there is a three-dimensional complex flow. Because of the cone-and-plate geometry, the fluid has a mean velocity that is a function of its position in the gap. The fluid flowing around the obstacle is submitted to an elongation behind the obstacle. The reason for this elongation is that the velocity at the sphere wall is zero and that the fluid must reach the mean velocity of the fluid in a certain distance. The first point is that the elongation is a function of the vertical position along the obstacle. Because the diameter of the obstacle is smaller than the gap distance, there is in addition a flow above the obstacle. All these apparent complex features do not in fact cause many difficulties. The main reason is that the flow above the obstacle does not introduce a noticeable perturbation to the features arising from the flow around the obstacle, in which we are interested. Moreover, as stressed in ref 13, we checked that all the phenomena due to the presence of the obstacle are located in a zone (shown as a shaded area in Figure 1) where it is possible to be away both from the perturbations caused by the plate wall and from the flow above the obstacle. We took as the representative elongation rate in the shaded area the one corresponding to the midpoint between the cone and the plate, which corresponds to the first third of the shaded area.

Results and Discussion

As said in the previous paragraph, the cone-and-plate geometry implies that there is a shear between the cone and the plate, with or without the presence of the obstacle. We know that above a certain critical shear rate, a band texture will appear after cessation of flow. Since we are interested in the texture that might appear behind the obstacle due to the elongation, we performed all the experiments at a shear rate less than the critical shear rate ($\dot{\gamma} < 1.1\ s^{-1}$ (ref 5)).

1. During the Flow. When an anisotropic solution flows around the obstacle, the most noticeable feature is the presence of a wake behind the obstacle. This wake is very long, more than 6 mm in length (the diameter of the obstacle being 250 μm). It is clearly visible because its birefringence is greater than the mean birefringence of the surrounding region (see Figure 3a in ref 13). The

0024-9297/91/2224-5683$02.50/0 © 1991 American Chemical Society

elongation phenomenon occurs within the wake. We will first measure the difference in birefringence between the wake and its surroundings and then quantify the elongation rate.

1.1. Wake Birefringence. In a cone-and-plate geometry, the retardation is a function of the position along the radius and of the birefringence of the sample. This birefringence is a complex function of the texture of the sample, the concentration, and the flow rate. We thus quantified a relative birefringence, which is the ratio of the birefringence in the wake (Δn_{wake}) over the birefringence (Δn_0) that the solution would have at the same place, but without the obstacle (and thus without elongation).

A sample with a uniform birefringence (Δn_0) (viewed between crossed polarizers with a white light) appears colored. This color is related to the optical path difference or retardation

$$\delta = z\Delta n_0$$

where z is the thickness of the sample and Δn_0 is the birefringence. In a cone-and-plate geometry, where the thickness varies linearly along a radius, this results in the observation of a determined color sequence called Newton's color sequence.[16] If somewhere in the sample (zone A) the birefringence (Δn_A) is different from the surrounding fluid (zone B) birefringence (Δn_0), the color sequence is then disturbed. If we note δ_A, the retardation through the zone A, locating the same color (in zone B) enables us to determine the relative birefringence:

$$\delta_A = \delta_B \quad \text{(same color)}$$

which means

$$z_A\Delta n_A = z_B\Delta n_0$$

which leads to

$$\Delta n_A/\Delta n_0 = z_B/z_A$$

The case of the wake is slightly more complicated because the wake is not observed throughout the whole thickness (z_A) of the fluid but only throughout the obstacle depth ($\phi_{obstacle}$). The fluid above this depth is supposed to have the same birefringence (Δn_0) as the surrounding fluid (see Figure 1). We then assume that the retardation of the light through z_A can be written as

$$\delta_A = \phi_{obstacle}\Delta n_{wake} + (z_A - \phi_{obstacle})\Delta n_0$$

This equation gives a very crude approximation of the actual retardation, but we believe it is enough to draw meaningful conclusions. Using the same procedure as in the previous case enables us to evaluate $\Delta n_{wake}/\Delta n_0$. The results are the following:

just behind the obstacle

$$\Delta n_{wake}/\Delta n_0 = 1.34$$

in the wake, 3 mm after the obstacle

$$\Delta n_{wake}/\Delta n_0 = 1.1$$

It appears that the wake is much more birefringent than the surrounding fluid and that this higher birefringence in the wake decreases with the distance from the obstacle. This increase of birefringence reflects an increase of orientation due to a better director alignment and/or molecular orientation.

1.2. Computation and Measurement of the Elongational Rate. The elongational rate was estimated with the help of tracers. The velocity of tracers was measured at different points in the wake (the method being discussed elsewhere[15]). The elongation rate is deduced from this. The results are given in Figure 2.

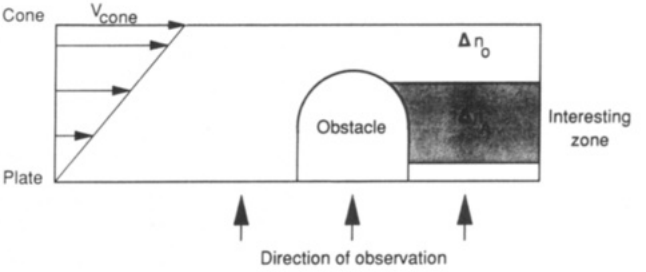

Figure 1. Location of the obstacle in the velocity field. The shaded area is where the elongation flow is the most preponderant.

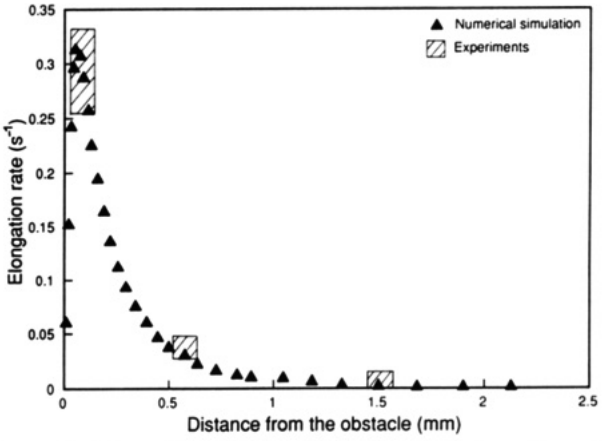

Figure 2. Elongation rates applied to the fluid along the wake for a mean fluid velocity of 0.08 mm/s. Comparison between experimental measurements and numerical predictions.

The elongation rate has a maximum near the obstacle and decreases along the wake. It was difficult to obtain accurate measurements close to the obstacle since we measured the velocity as the time needed by a tracer to travel a certain distance. This explains the large error committed at this point.

A numerical simulation was performed with a power law equation. The simulation used a two-dimensional finite element code developed in the laboratory.[17] The aim was to see if there is an agreement between the numerical prediction and our measurements.

The comparison is reported in Figure 2. We can notice a good agreement with the power law simulation. Although the power law is a simple way of simulating the behavior of such a fluid, the numerical calculations predict quite accurately the elongation. Therefore the numerical simulation will be used to give the elongation rate applied to the fluid. Hereafter we will always speak of the maximum elongation rate applied to the fluid ($\dot{\alpha}_{max}$) (see in Figure 2).

1.3. Discussion. We can summarize the observations about the wake and the numerical predictions as follows (Figure 3):

(i) Behind the obstacle, the fluid is subjected to an elongation rate ($\dot{\alpha}_{max}$) that results in a higher degree of orientation compared to the surrounding fluid, despite that the deformation is small (an estimate of the deformation submitted to the fluid during the elongation gives less than three strain units) compared to what is needed in shear.[5,6,18,19]

(ii) When the fluid moves away from the obstacle, the elongation slowly vanishes, but the small amount of elongation still present is nevertheless sufficient to keep the high degree of orientation previously induced by the maximum elongation rate.

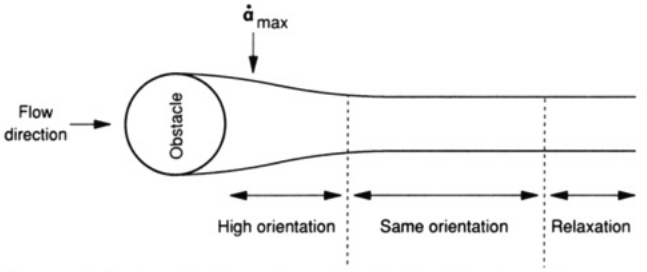

Figure 3. Induced orientation of the fluid arising from the elongational flow.

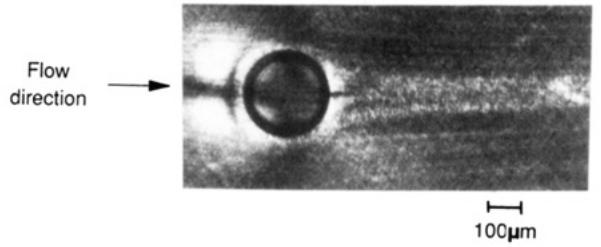

Figure 4. Optical micrograph taken after cessation of flow ($\dot{\gamma}$ = 0.3 s^{-1}) when the band texture is completely formed.

Chart I

flow conditions	resulting texture in the wake after cessation of flow
$\dot{\alpha}_{max} < 0.05\ s^{-1}$	wake is visible but bands never appear in it
$\dot{\alpha}_{max} = 0.05\ s^{-1}$	indefinite texture is observed in the wake
$\dot{\alpha}_{max} = 0.08\ s^{-1}$	bands appear in the first part of the wake (2 mm in length just behind the obstacle); in the second part, the wake is always visible but no texture is observed
$\dot{\alpha}_{max} > 0.08\ s^{-1}$	bands appear in the whole wake (which means the visible part of the wake with our setup, i.e., 6 mm in length)

(iii) Two millimeters further on, the elongation rate is reduced to zero. The fluid in the wake is then only submitted to the same shear rate as the surrounding fluid, and thus it tends to relax. One particular feature about the liquid crystalline polymers is that the birefringence relaxation is quite long. This explains the length of the wake.

2. Relaxation. When the flow is stopped, no special texture appears in the field of view away from the obstacle since the shear rate is less than the critical shear rate. But in the vicinity of the obstacle, bands might form in two locations (Figure 4): (i) around the obstacle and (ii) in the wake. Since the flow in the wake is mainly elongational, we will focus our attention on the appearance of bands in the wake and particularly investigate the elongation conditions for the formation of a band texture after cessation of flow.

2.1. Flow Conditions for the Formation of the Band Texture. Depending on the flow conditions (that is, the maximum elongation rate applied to the fluid (see paragraph 1.2)), a band texture will or will not appear in the wake after cessation of flow. Chart I summarizes the results. The results show that, after cessation of flow, bands only appear when the maximum elongation rate ($\dot{\alpha}_{max}$) is larger than a critical value ($\dot{\alpha}_c$), which in our case is about 0.05 s^{-1}. So in both cases, either a shear or an elongation, there is a critical flow rate above which bands will form when the flow is stopped. Comparing the critical elongation rate ($\dot{\alpha}_c$ = 0.05 s^{-1}) and the critical shear rate ($\dot{\gamma}_c$ = 1.1 s^{-1}) for the same material, we can see that an elongation is much more efficient than a shear to see bands form after cessation of flow.

It should be noted that the applied elongation strain is small compared to the large value required for shear ($\alpha > 100$). The large difference between $\dot{\gamma}_c$ and $\dot{\alpha}_c$ can be appreciated considering that the elongation is in the flow direction, contrary to a shear which combines two disadvantages, a rotational component and an elongation component not in the flow direction.

Speaking now in terms of time for the appearance and the destruction of bands obtained after an elongation, we observed that (i) when the elongation rate is close to $\dot{\alpha}_c$ (but above it), bands appear a certain time after cessation of flow, and (ii) if we apply a higher elongation rate, bands form in the wake immediately after cessation of flow. Identical results were found in the case of a shear, and a comparison of the lifetimes of bands in both cases shows that they are of the same order of magnitude. (Their lifetime is on the order of minutes and depends on the previously applied flow rate.[6])

Thus the existence, in both cases, of a critical flow rate for the formation of bands and a similar time scale for their appearance, lifetime, and destruction shows that the mechanisms of formation of bands are identical after a shear or an elongation.

As the mechanisms for the formation of bands after a shear or after an elongation seemed identical, it was interesting to complete the study by checking whether the formed bands were identical or not.

2.2. Optical Properties of the Bands. Optical properties of bands have been extensively described,[1-3] particularly the shifting of the black lines when the crossed polarizers rotate. Because of our setup, where the position of the sample is fixed and where the analyzer can only be placed in two positions ($\theta = 0°$ and $\theta = 45°$), the optical properties were only investigated for these two angles.

Both bands after a shear and bands after an elongation can be studied with our setup: after a shear, bands appear (when the shear rate is higher than the critical shear rate (1.1 s^{-1})) in the field of view away from the obstacle; after an elongation, bands appear in the wake when the elongation rate is higher than the critical elongation rate (0.05 s^{-1}). One way to characterize a band texture is to measure the band spacing.

The results are as follows:

θ	band spacing, μm
after a shear	
$\theta = 0°$	7 ± 1
$\theta = 45°$	12 ± 1
after an elongation	
$\theta = 0°$	6 ± 1

Because of the blurred texture when $\theta = 45°$ no measurement could be performed in the wake. But we can see that, in the shear case, the spacing when $\theta = 45°$ is twice the spacing when $\theta = 0°$, as expected.[3]

Different shear rates and different elongation rates were investigated but no influence of the flow rates on the band spacing could be noticed, which confirms previous works.[5,9]

It appears that, for the same polymer, the band spacing is similar after a shear or after an elongation and is also independent of the flow rate, which means that (1) bands, which appear after a shear or an elongation, are identical

and (2) the band properties do not depend on the previous flow conditions.

Conclusion

Studying an elongational flow, resulting from the presence of an obstacle, is an instructive way of investigating the behavior of a liquid crystalline polymer. This way of producing an elongational flow is not ideal because the elongation rate is not uniform in the whole field. Despite this, this setup enables us to give some first quantitative results about the behavior of a liquid crystalline polymer when submitted to an elongation and during the relaxation.

Our results confirm that an elongation is more efficient than a shear to orientate a liquid crystalline polymer.

Concerning the occurrence of bands after an elongational flow during the relaxation, it appears that there is a critical elongation rate below which no band appears and above which bands form. An identical condition has already been found in the case of a shear. Other similarities between the bands obtained after an elongation and after a shear were also noticed: (i) similar time periods, whether we speak about the time for their appearance or their lifetime, and (ii) totally identical bands after a shear or after an elongation. All these results show that the relaxation modes are identical after a shear or an elongation, that is, whatever the previous flow may be. Secondly, we saw that the band properties are not controlled at all by the previous flow conditions, which implies that they must be controlled by characteristic parameters of the fluid, probably a combination of elastic constants.

References and Notes

(1) Viney, C.; Donald, A. M.; Windle, A. H. *J. Mater. Sci.* **1983**, *18*, 1136.
(2) Donald, A. M.; Windle, A. H. *J. Mater. Sci.* **1983**, *18*, 1143.
(3) Navard, P.; Zachariades, A. E. *J. Polym. Sci., Polym. Phys. Ed.* **1987**, *25*, 1089.
(4) Marsano, E.; Carpanato, L.; Ciferri, A. *Mol. Cryst. Liq. Cryst.* **1988**, *158*, 267.
(5) Ernst, B. Thèse de Doctorat, "Rhéologie et rhéo-optique des solutions mésomorphes d'hydroxypropylcellulose", Ecole Nationale Supérieure des Mines de Paris, 1989.
(6) Ernst, B.; Navard, P. *Macromolecules* **1989**, *22*, 1419.
(7) Takabe, T.; Hashimoto, T.; Ernst, B.; Navard, P.; Stein, R. S. *J. Chem. Phys.* **1990**, *92*, 1386.
(8) Ernst, B.; Navard, P.; Hashimoto, T.; Takebe, T. *Macromolecules* **1990**, *23*, 1370.
(9) Fincher, C. R. *Mol. Cryst. Liq. Cryst.* **1988**, *155*, 559.
(10) Dobb, M. G.; Johnson, D. J.; Saville, B. P. *J. Polym. Sci., Polym. Phys. Ed.* **1977**, *15*, 2201.
(11) Horio, M.; Ishikawa, S.; Oda, K. *J. Polym. Sci., Appl. Polym. Symp.* **1985**, *41*, 269.
(12) Peuvrel, E. Thèse de Doctorat, "Ecoulement de cristaux liquides polymères autour d'obstacles—Application aux composites", Ecole Nationale Supérieure des Mines de Paris, 1990.
(13) Peuvrel, E.; Navard, P. *Liq. Cryst.* **1990**, *7*, 95.
(14) Cressely, R.; Hocquart, R. *Opt. Acta* **1980**, *27*, 699.
(15) Peuvrel, E.; Navard, P. *Macromolecules* **1990**, *23*, 4874.
(16) Haudin, J. M. In *Optical Properties of Polymers*; Meeten, G. H., Ed.; Elsevier Applied Science Publishers: London, 1986; Chapter 4.
(17) Cescutti, J. P. Thèse de Doctorat, "Contribution à la Simulation Numérique du Forgeage", Ecole Nationale Supérieure des Mines de Paris, 1989.
(18) Picken, S. J.; Aerts, J.; Visser, R.; Northolt, M. G. *Macromolecules* **1990**, *23*, 3849.
(19) Moldenaers, P.; Fuller, G.; Mewis, J. *Macromolecules* **1989**, *22*, 960.

Registry No. (Hydroxypropyl)cellulose, 9004-64-2.